

Check for updates



Ultrasonographic Analysis of Site-Specific Plantar Skin Thickness for Melanoma Staging and Excision

Jiin $\operatorname{Kim}^1 \bigcirc \mid \operatorname{Subin} \operatorname{Hur}^1 \bigcirc \mid \operatorname{Kyu-Lim} \operatorname{Lee}^2 \bigcirc \mid \operatorname{Hee-Jin} \operatorname{Kim}^{2,3} \bigcirc$

¹Department of Medical Sciences 2nd Grade, Chonnam National University, Hwasun-gun, Jeonnam, Republic of Korea | ²Division in Anatomy and Developmental Biology, Department of Oral Biology, Human Identification Research Institute, BK21 FOUR Project, Yonsei University College of Dentistry, Seoul, South Korea | ³Department of Materials Science & Engineering, College of Engineering, Yonsei University, Seoul, South Korea

Correspondence: Kyu-Lim Lee (kyulimlee@yuhs.ac) | Hee-Jin Kim (hjk776@yuhs.ac)

Received: 21 May 2025 | Revised: 13 July 2025 | Accepted: 16 July 2025

Keywords: Breslow thickness | high-frequency ultrasound | plantar melanoma | skin thickness | surgical excision margins

ABSTRACT

Plantar melanomas present unique diagnostic and surgical challenges owing to substantial regional variations in skin thickness. Although the Breslow thickness remains the primary criterion for staging and surgical excision, its application on plantar melanoma is complicated by the inherent thickness of the glabrous plantar epidermis, which may lead to tumor depth overestimation. Accurate assessment of plantar skin thickness is essential for optimizing staging accuracy and refining surgical margins. This study aimed to investigate plantar epidermal, dermal, and total skin thicknesses at 14 anatomical locations using high-frequency ultrasonography (HFUS) and histological analysis. A total of 35 ft (27 from cadavers and eight from patients) were examined. Mean total skin thickness was 1.71 ± 0.31 mm, although mean epidermal thickness was 0.55 ± 0.12 mm and mean dermal thickness was 0.55 ± 0.12 mm and 0.55 ± 0.12 mm and 0ness was 1.16 ± 0.27 mm. Significant regional variations were observed (p < 0.05), with the heel (S11) exhibiting the greatest thickness $(2.19 \pm 0.29 \,\mathrm{mm})$ and the medial arch (S4) the least $(1.41 \pm 0.26 \,\mathrm{mm})$. The results also included thickness ranking in order of the heel, forefoot, lateral arch, and medial arch. These findings suggest that plantar skin thickness correlates with mechanical stress distribution, with weight-bearing regions exhibiting greater epidermal and dermal thicknesses. By providing a comprehensive dataset of site-specific plantar skin thicknesses, this study enhances the precision of ultrasonographic melanoma assessment, refines tumor staging, and aids in optimizing excision margins. These findings offer clinically relevant anatomical reference points that may improve surgical decision-making, minimize unnecessary excisions, and enhance the prognosis of melanoma. Further studies should explore the correlation between ultrasonographic and histopathological measurements across diverse populations to strengthen their clinical applicability.

1 | Introduction

Melanoma is an aggressive malignancy that originates from melanocytes, with cutaneous melanoma being the most common subtype primarily associated with exposure to ultraviolet (UV) radiation (Loscalzo et al. 2022). In contrast, acral melanoma, which occurs in glabrous skin, such as the palms, soles, and subungual regions, is not linked to UV exposure, but is

associated with mechanical stress, including chronic pressure and shear forces (Gui et al. 2022; Brunicardi et al. 2019). Several studies suggest that mechanical stress in weight-bearing plantar regions may contribute to tumor development by modifying the skin microenvironment (Minagawa et al. 2016). Prolonged exposure to pressure and shear forces can induce keratinocyte hypertrophy, extracellular matrix remodeling, and changes in cellular adhesion, thereby promoting tumor progression by

Jiin Kim and Subin Hur contributed equally to this work.

This is an open access article under the terms of the Creative Commons Attribution-NonCommercial-NoDerivs License, which permits use and distribution in any medium, provided the original work is properly cited, the use is non-commercial and no modifications or adaptations are made.

© 2025 The Author(s). Clinical Anatomy published by Wiley Periodicals LLC on behalf of American Association of Clinical Anatomists and British Association of Clinical Anatomists.

facilitating invasion and increasing metastatic potential (Seo et al. 2022). Consequently, plantar melanoma has a higher incidence in weight-bearing areas, such as the central heel, inner forefoot, and outer midfoot, where the unique skin structure and pressure gradients may create a favorable environment for tumor invasion (Jung et al. 2013).

Tumor staging plays a crucial role in prognostic evaluation and therapeutic decision-making (Loscalzo et al. 2022). The TNM classification remains the most widely adopted system for melanoma classification, with the T classification based on the Breslow thickness (Table 1) (Fischer 2019; Boland and Gershenwald 2016). For treatment, a wide local excision should be performed with an adequate margin and depth, including the normal skin comprising the epidermis, dermis, and subcutaneous fat (Koshenkov et al. 2016). The excision margin for melanoma resection is determined based on the Breslow thickness, which measures the vertical depth of tumor invasion from the granular layer of the epidermis (Long et al. 2023). Therefore, precisely determining surgical margins according to lesion thickness is critical for optimizing patient outcomes (Avry et al. 2022).

High-frequency ultrasonography (HFUS) has emerged as a valuable non-invasive imaging tool for assessing tumor thickness and guiding clinical decision-making in melanoma. HFUS has demonstrated high accuracy in detecting tumor depth, particularly in the sole of the foot, compared with other body areas (Hayashi et al. 2009). By enabling high-resolution imaging of the skin from the stratum corneum to the deep fascia (Levy et al. 2021), HFUS allows clear visualization of skin layers and deeper structures. On ultrasound imaging, melanomas typically appear as well-demarcated, fusiform, homogeneous, and hypoechoic lesions (Avry et al. 2022). The reliability of HFUS on tumor depth evaluation facilitates precise surgical planning, optimal margin selection, and reduces surgical risk while improving cosmetic outcomes, showing a strong correlation between histological Breslow thickness and sonographic measurements (Avry et al. 2022; Levy et al. 2021; Sellyn et al. 2025).

Establishing normative data on plantar skin thickness is essential for optimizing the assessment and prognosis of ultrasonographic melanoma. The plantar skin has a unique anatomical structure with substantial regional variations in thickness compared with other body areas (Fischer 2019; Levy et al. 2021; Chao et al. 2011). However, previous studies have provided limited data, often reporting a single representative value for the

TABLE 1 | T classification of melanoma and recommended surgical margins for local excision based on the Breslow thickness.

Breslow thickness	T classification	Surgical margin
In situ	Tis	0.5-1 cm
≤1 mm	T1	1.0 cm
1.01-2.00 mm	T2	1-2 cm
2.01-4.00 mm	Т3	2 cm
>4.0 mm	T4	2 cm

entire skin and epidermal layer (Lee and Hwang 2002; Lintzeri et al. 2022) or focusing on restricted regions such as the heel, forefoot, and toes (Chao et al. 2011; Morrison et al. 2021). Additionally, many studies rely solely on ultrasound, with a few employing multiple imaging and measurement techniques, resulting in a lack of comprehensive and precise assessments of plantar skin and epidermal thickness.

To address this gap, the present study conducted an extensive assessment of plantar skin thickness across multiple anatomical regions of the foot using ultrasonography and histology. Furthermore, we aimed to enhance the clinical applicability of our findings by incorporating multiple easily palpable and clinically relevant anatomical landmarks (Hashmi et al. 2015; Campillo-Recio et al. 2021). Given the significant variability in plantar skin thickness and the clinical importance of accurately determining tumor depth and the skin layer that melanoma invades (Machet et al. 2009), a thorough understanding of regional skin thickness is essential in improving melanoma prognosis, refining therapeutic strategies, and optimizing surgical excision planning.

2 | Materials and Methods

This study examined 35 ft, including 17 from males (mean age: 78.1 years) and 18 from females (mean age: 68.8 years), with an overall mean age of 73.5 years. The specimens were categorized into formalin-embalmed cadaveric feet (type 1, n=18), fresh cadaveric feet (type 2, n=9), and feet of living patients (type 3, n=8). The cadavers were donated to the Yonsei Medical Center (Seoul, Republic of Korea) and dissected with authorization from the Surgical Anatomy Education Center at the Yonsei University College of Medicine. For the patient dataset, ultrasonographic images of individuals who underwent routine foot examinations were retrospectively analyzed. No additional imaging was performed, and only records from patients without dermatological or systemic conditions affecting skin thickness were included. This study was a retrospective analysis of anonymized clinical data.

2.1 | Ultrasound Examination and Measurement Protocol

The 14 anatomical measurement sites included the middle of the first, third, and fifth toes (P1–P3), the sesamoid of the first metatarsal bone (S1), the head of the fifth metatarsal bone (S3), the navicular region (S7), the base of the fifth metatarsal bone (S9), the heel center meeting the vertical line of the lateral malleolus (S10), and the calcaneal tuberosity (S11). Additional midpoints (S2, S4, S5, S6, and S8) were defined based on anatomical relevance; the middle of S1 and S3 (S2), the middle of S1 and S7 (S4), the middle of S4 and S6 (S5), the middle of S3 and S9 (S6), and the middle of S7 and S9 (S8) (Figure 1).

Ultrasound imaging was performed at 14 predefined anatomical sites on the plantar surface using a high-frequency 18 MHz linear transducer ultrasound system (Sonimage HS1; KONICA MINOLTA, Tokyo, Japan). Image depth was set to 2cm for P1–P3 and S1–S9, and 3.5cm for S10–S11. The transducer was

2 Clinical Anatomy, 2025

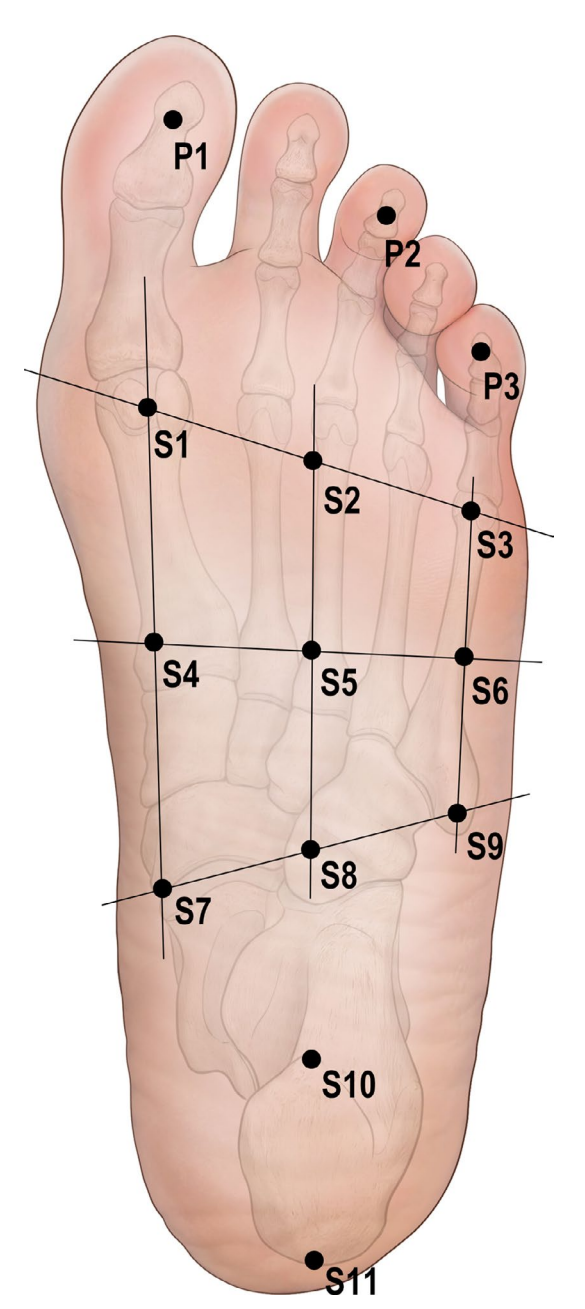


FIGURE 1 | Eleven plantar anatomical measurement sites used in this study; (P1) middle of the first toe; (P2) middle of the third toe; (P3) middle of the fifth toe; (S1) the sesamoid of the first metatarsal bone; (S2) middle of S1 and S3; (S3) head of the fifth metatarsal bone; (S4) middle of S1 and S7; (S5) middle of S4 and S6; (S6) middle of S3 and S9; (S7) the navicular region; (S8) middle of S7 and S9; (S9) base of the fifth metatarsal bone; (S10) the heel center meeting with the vertical line of the lateral malleolus; (S11) the calcaneal tuberosity.

positioned perpendicular to the plantar surface, and a water-soluble gel (SONO JELLY, MEDITOP Corporation, Youngin, Korea) was used to optimize contact and minimize compression artifacts.

Two examiners independently acquired ultrasound images and measured the skin and epidermal thicknesses at each site using ImageJ software (National Institutes of Health, Bethesda, MD, USA). Dermal thickness was calculated by subtracting the epidermal thickness from the total skin thickness. Each measurement

was repeated three times, and the final values were determined as the average of the two examiners' measurements.

To validate the accuracy of the ultrasonographic measurements, a specialized anatomist performed a layer-by-layer dissection of the cadaveric specimens. Epidermal and dermal thicknesses were directly measured using high-precision calipers and compared with ultrasonographic data to confirm the correspondence between ultrasound imaging and actual anatomical structures.

2.2 | Histological Examination

To further assess skin thickness, histological analysis was performed on the skin and subcutaneous fat samples obtained from three key sites (S1, S4, and S10). Collected tissue samples were routinely embedded in paraffin and processed for hematoxylin and eosin (H&E) and Masson's trichrome staining. Sections from each formalin-fixed, paraffin-embedded block were stained with undiluted Harris hematoxylin and 0.5% eosin for detailed microscopic evaluation of the epidermal and dermal structures. Masson's trichrome staining was performed using the Harris hematoxylin and aniline blue to further investigate the collagen fibers in the dermis.

2.3 | Statistical Analysis

All statistical analyses were performed using SPSS (software version 23.0; IBM, Armonk, NY, USA). Statistical significance was set at p < 0.05. To evaluate differences between groups, the student's t-test was used to compare measurement values based on sex, laterality, and sample type. Analysis of variance was performed to examine variations among different plantar points and between cadavers and living individuals. Additionally, a correlation analysis was conducted to assess the relationship between age and measurement values.

3 | Results

3.1 | Ultrasonographic and Histological Findings

In the ultrasonographic images, the epidermis appeared as a distinct hyperechoic double layer with a subepidermal low-echogenic band (SLEB) beneath it, representing the papillary dermis. Below the SLEB, the reticular dermis appeared as a hyperechoic structure with lower brightness than the epidermis. The subcutaneous tissue was clearly distinguishable from the dermis, appearing as hypoechoic fat lobules separated by thin hyperechoic septa.

Histological examinations were performed in three major anatomical regions (S1, S4, and S10) and compared with the ultrasound images (Figure 2). H&E staining confirmed that the epidermis comprised a stratified squamous epithelial layer, whereas the papillary dermis exhibited loose connective tissue with relatively low collagen density. The reticular dermis contained dense collagen fibers corresponding to the hyperechoic signal observed during ultrasonography. The subcutaneous tissue displayed a lobular architecture of adipose tissue, with

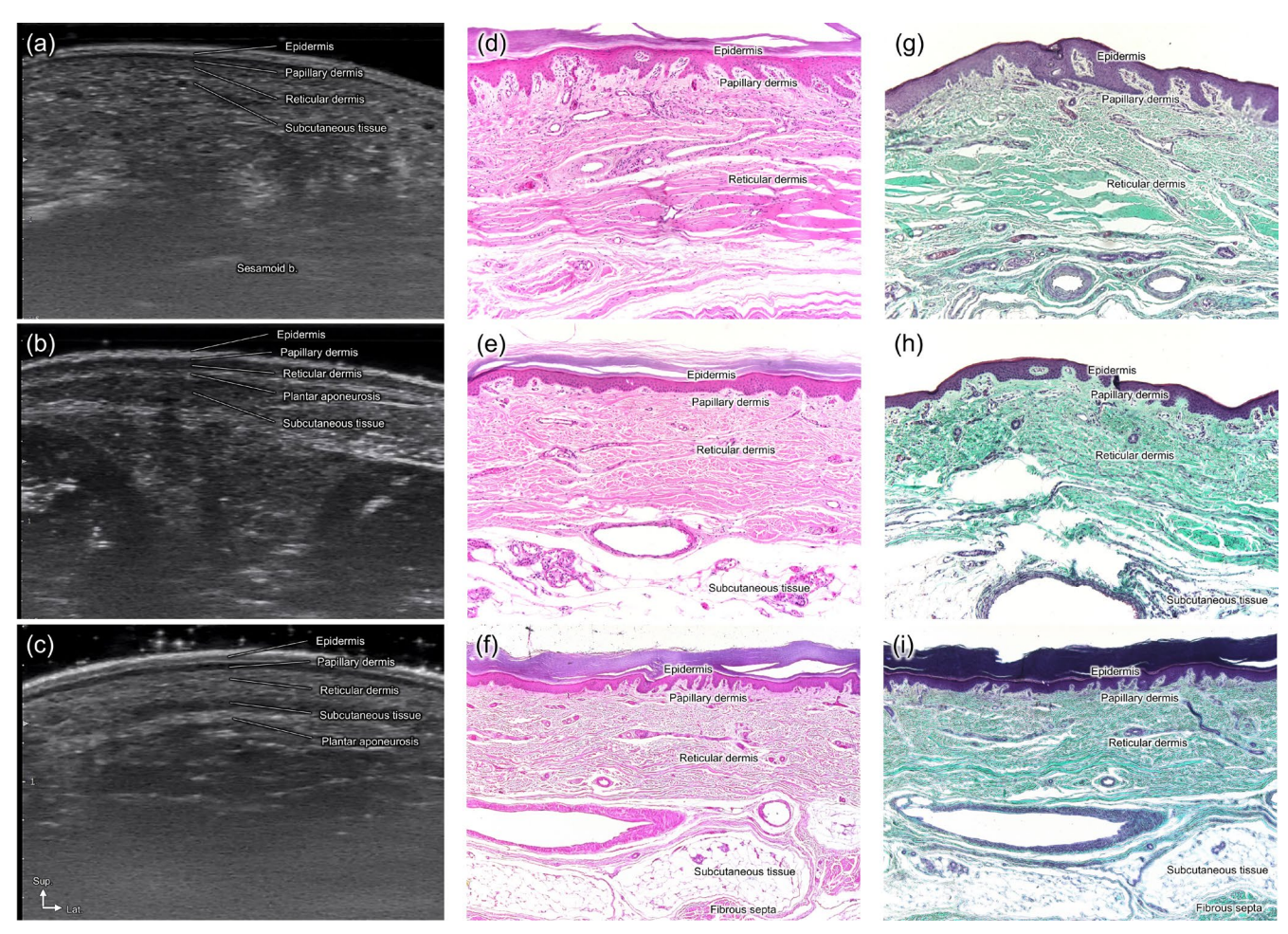


FIGURE 2 | US images, H&E stain, and the Masson's trichrome stain of three major anatomical regions: S1 (a, d, g), S4 (b, e, h), and S10 (c, f, i). The US images (a-c) confirm the epidermis, papillary and reticular dermis, subcutaneous tissue, and plantar aponeurosis, each exhibiting distinct echogenicity. The H&E stains (d, e: \times 10; f: \times 5) clearly define the microstructures from the epidermis to the subcutaneous tissue, correlating with the US images. The Masson's trichrome stains (g, h: \times 10; i: \times 5) highlight collagen fibers within the dermal layer and fibrous septa in blue.

interspersed fibrous septa. These histological characteristics correspond well with the ultrasound images, thereby validating the structural layers observed in the ultrasonographic assessment.

The Masson's trichrome staining highlighted a well-organized arrangement of loose and dense connective tissues in the dermal layers, primarily comprising collagen fibers. Additionally, it confirmed fibrous septa within the subcutaneous fat layer, which were particularly prominent in specific regions such as S10.

3.2 | Skin Thicknesses at Fourteen Points Using US Measurements

The epidermal and total skin thicknesses at the 14 plantar measurement points are presented in Tables 2 and 3. Skin thickness, including both epidermal and dermal layers, was between 1.41 to 2.05 mm, with an average of 1.71 ± 0.31 mm (mean \pm standard deviation). Epidermal thickness varied from 0.43 to 0.71 mm, with an average of 0.55 ± 0.12 mm. Both skin and epidermal thicknesses differed significantly among the plantar regions (p < 0.05). The heel (S10 and S11) exhibited the greatest total skin and epidermal thicknesses, followed by the forefoot

(S1–S3), lateral arch (S6 and S9), and medial arch (S4, S5, S7, and S8) (Figure 3). The toe regions (P1–P3) showed thickness values comparable with those of the forefoot, lateral arch, and medial arch, with notable variations among individual toes.

Statistical analysis revealed that dermal thickness was significantly greater in males than in females (p < 0.05; Table 2), whereas the total skin and epidermal thicknesses showed no significant sex-related differences. Comparisons between sample types (cadaveric vs. living) demonstrated significant differences in epidermal thicknesses (p < 0.05; Table 3), whereas total skin and dermal thicknesses remained comparable across the groups. Correlation analyses between age and thicknesses did not yield statistically significant correlation coefficients, and no laterality differences were observed between the left and right feet. Results without statistical significance were not presented.

4 | Discussion

The plantar skin is structurally adapted for weight-bearing, featuring a thickened epidermis with hypertrophic keratinocytes interdigitating with the papillary dermis (Boyle et al. 2019; Fuchs et al. 2024). The arch structure of the foot

4 Clinical Anatomy, 2025

 TABLE 2
 Soft tissue thickness of each layer of the skin at measurement points: comparison between sexes.

		P1	P2	P3	S1	S2	S3	S4	SS	98	S7	88	68	S10	S11
Epidermis		Total 0.54 ± 0.08 0.51 ± 0.07 0.49 ± 0.09 0.57 ± 0.10	0.51 ± 0.07	0.49 ± 0.09	0.57 ± 0.10	0.57 ± 0.10	0.61 ± 0.10	0.44 ± 0.08	0.44 ± 0.08 0.46 ± 0.08 0.53 ± 0.08	0.53 ± 0.08	0.49 ± 0.10	0.54 ± 0.10 0.54 ± 0.10 0.70 ± 0.13	0.54 ± 0.10	0.70 ± 0.13	0.69 ± 0.16
	Male	0.53 ± 0.09	0.51 ± 0.08 0.48 ± 0.10 0.58 ± 0.11	0.48 ± 0.10	0.58 ± 0.11	0.57 ± 0.11	0.59 ± 0.10	0.45 ± 0.10	0.45 ± 0.07 0.51 ± 0.07		0.46 ± 0.09	0.54 ± 0.10	0.53 ± 0.11	0.71 ± 0.12	0.67 ± 0.13
	Female	Female 0.55 ± 0.08 0.52 ± 0.07 0.50 ± 0.09 0.57 ± 0.08	0.52 ± 0.07	0.50 ± 0.09	0.57 ± 0.08	0.57 ± 0.09	0.63 ± 0.11	0.42 ± 0.07	0.47 ± 0.09	0.56 ± 0.09	0.51 ± 0.11	0.54 ± 0.10	0.56 ± 0.10	0.70 ± 0.15	0.71 ± 0.19
Dermis*	Total	Total 1.24 ± 0.22 1.20 ± 0.18 1.08 ± 0.21 1.18 ± 0.21	1.20 ± 0.18	1.08 ± 0.21	1.18 ± 0.21	1.31 ± 0.24	1.16 ± 0.22	0.97 ± 0.23 1.02 ± 0.18	1.02 ± 0.18	1.13 ± 0.20	1.03 ± 0.18	1.04 ± 0.19	1.09 ± 0.22	1.35 ± 0.35	1.50 ± 0.30
	Male	1.27 ± 0.22	1.26 ± 0.20 1.13 ± 0.24 1.21 ± 0.17	1.13 ± 0.24	1.21 ± 0.17	1.40 ± 0.18	1.22 ± 0.18	0.98 ± 0.27	1.02 ± 0.19	1.20 ± 0.20	1.05 ± 0.19	1.10 ± 0.20	1.07 ± 0.21	1.37 ± 0.40	1.47 ± 0.31
	Female	Female 1.20±0.23	1.13 ± 0.13	1.02 ± 0.18	1.14 ± 0.24	1.21 ± 0.27	1.09 ± 0.23	0.97 ± 0.17	1.02 ± 0.17	1.05 ± 0.17	1.00 ± 0.17	0.97 ± 0.16	1.11 ± 0.22	1.34 ± 0.31	1.54 ± 0.30
Skin	Total	1.77 ± 0.22	1.71 ± 0.18 1.57 ± 0.21 1.75 ± 0.22	1.57 ± 0.21	1.75 ± 0.22	1.88 ± 0.24	1.77 ± 0.25	1.41 ± 0.26	1.48 ± 0.21	1.66 ± 0.20	1.51 ± 0.18	1.58 ± 0.21	1.63 ± 0.26	2.06 ± 0.38	2.19 ± 0.29
	Male	1.80 ± 0.23	1.80 ± 0.23 1.77 ± 0.20 1.62 ± 0.22 1.78 ± 0.17	1.62 ± 0.22	1.78 ± 0.17	1.97 ± 0.17	1.81 ± 0.19	1.43 ± 0.31 1.47 ± 0.22		1.70 ± 0.21	1.51 ± 0.23	1.64 ± 0.24	1.60 ± 0.23	2.08 ± 0.40	2.14 ± 0.29
	Female	Female 1.75 ± 0.21 1.65 ± 0.13 1.52 ± 0.20 1.71 ± 0.25	1.65 ± 0.13	1.52 ± 0.20	1.71 ± 0.25	1.78 ± 0.27	1.72 ± 0.30	1.39 ± 0.20 1.48 ± 0.21		1.60 ± 0.17	1.51 ± 0.12	1.51 ± 0.16	1.66 ± 0.29	2.03 ± 0.37	2.25 ± 0.30

Note: Data are presented as mean \pm standard deviation in millimeters; statistically significant differences between both genders. $^*p < 0.05$.

TABLE 3 | Epidermal thickness at measurement points: comparison between sample types.

S11	0.69±0.16	0.66 ± 0.15	0.81 ± 0.11
S10	$0.57 \pm 0.10 0.61 \pm 0.10 0.44 \pm 0.08 0.46 \pm 0.08 0.53 \pm 0.08 0.49 \pm 0.10 0.54 \pm 0.10 0.54 \pm 0.10 0.70 \pm 0.13 0.69 \pm 0.16 = 0.10 = 0.00 \pm 0.00 \pm 0.00 = 0.00 \pm 0.00 \pm 0.00 = 0.00 = 0.00 = 0.00 \pm 0.00 = $	$0.56 \pm 0.10 0.60 \pm 0.10 0.42 \pm 0.05 0.45 \pm 0.08 0.51 \pm 0.08 0.45 \pm 0.09 0.52 \pm 0.10 0.52 \pm 0.10 0.67 \pm 0.122 0.66 \pm 0.15 = 0.12 0.66 \pm 0.12 = 0.12 $	$0.61 \pm 0.07 0.67 \pm 0.12 0.51 \pm 0.13 0.50 \pm 0.04 0.60 \pm 0.05 0.59 \pm 0.05 0.60 \pm 0.05 0.62 \pm 0.05 0.82 \pm 0.12 0.81 \pm 0.11 $
6S	0.54 ± 0.10	0.52 ± 0.10	0.62 ± 0.05
88	0.54 ± 0.10	0.52 ± 0.10	0.60±0.05
S7	0.49±0.10	0.45 ± 0.09	0.59 ± 0.05
98	0.53 ± 0.08	0.51 ± 0.08	0.60 ± 0.05
SS	0.46±0.08	0.45 ± 0.08	0.50 ± 0.04
S4	0.44±0.08	0.42 ± 0.05	0.51 ± 0.13
S3	0.61 ± 0.10	0.60 ± 0.10	0.67 ± 0.12
S2		0.56 ± 0.10	0.61 ± 0.07
S1	0.57 ± 0.10	0.57 ± 0.10	0.61 ± 0.09
P3	0.49±0.09	0.48 ± 0.10	0.51 ± 0.06
P2	0.51 ± 0.07	0.50 ± 0.07	0.58 ± 0.05
P1	Epidermis* Total 0.54 ± 0.08 0.51 ± 0.07 0.49 ± 0.09 0.57 ± 0.10	$\begin{array}{llllllllllllllllllllllllllllllllllll$	Type 3 0.61 ± 0.10 0.58 ± 0.05 0.51 ± 0.06 0.61 ± 0.09
	Total	Type 1+ Type 2	Type 3
	Epidermis*		

Note: Data are presented as the mean \pm standard deviation in millimeters; statistically significant differences between types. *p < 0.05.

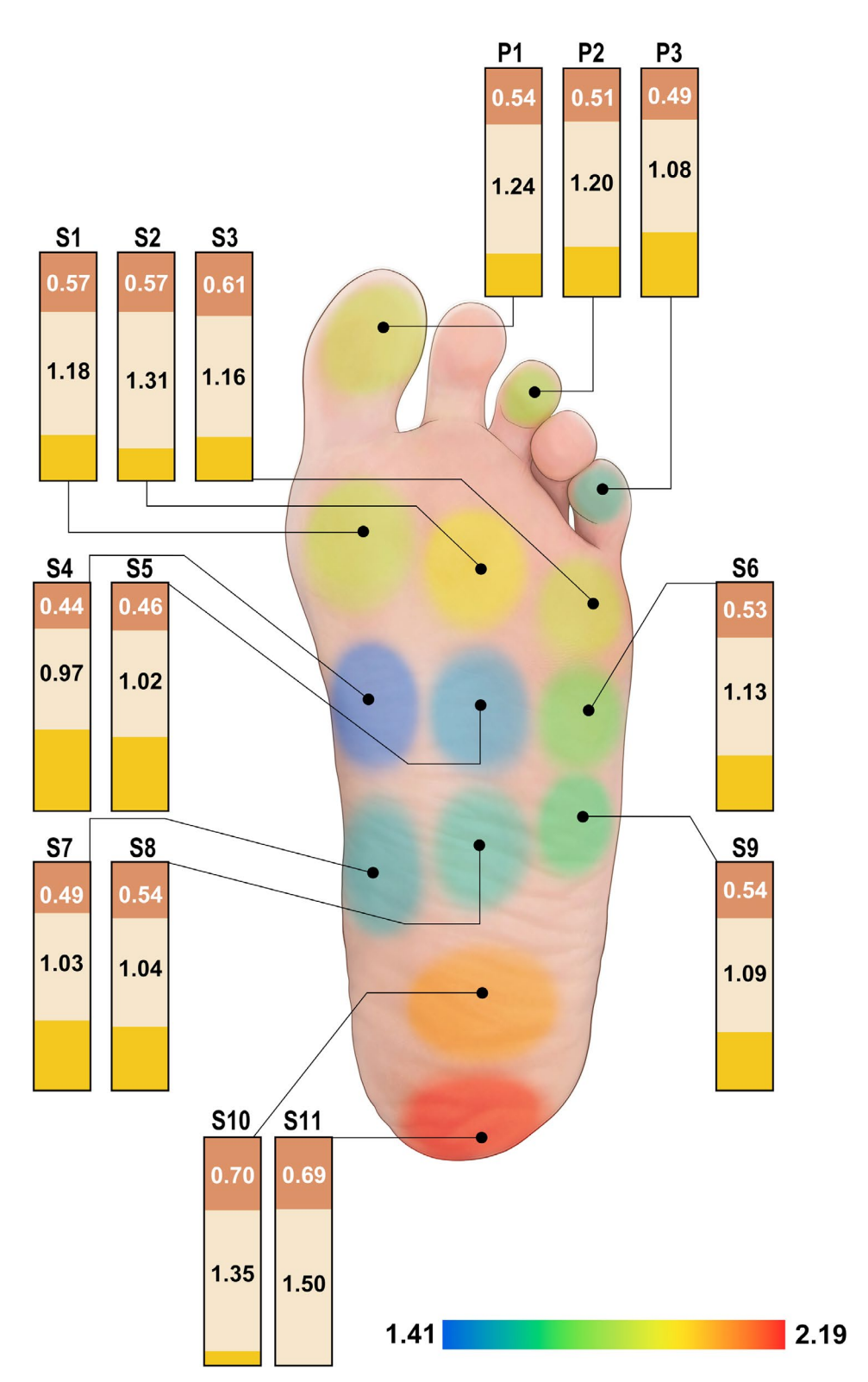


FIGURE 3 | Color scale indicates the thickness of the plantar skin and each measurement of the epidermal and dermal thicknesses. S4 was the thinnest site for both the epidermis and dermis, with an average epidermal thickness of 0.44 mm and dermal thickness of 0.97 mm. The thickest site of the epidermis was S10, measuring an average of 0.70 mm, while the thickest site of the dermis was S11, with an average thickness of 1.50 mm.

creates unequal mechanical stress, leading to regional variations in skin thickness (Van Boerum and Sangeorzan 2003), emphasizing the need for site-specific analysis. Melanoma excision requires a complete wide local excision (Rager et al. 2005); however, smaller margins are often used in the

plantar region because of limited skin mobility, which complicates primary closure (Loscalzo et al. 2022). Although no universal excision depth has been defined (DeFazio et al. 2010), current guidelines recommend fascia-level excision for invasive melanoma, whereas in situ melanoma is typically excised

with skin and subcutaneous fat to balance oncologic and functional outcomes (Lillemoe et al. 2023). The plantar epidermis is significantly thicker than other skin sites (Lee and Hwang 2002), which may cause the Breslow thickness-based T-staging to overestimate invasion depth, even in melanoma in situ (Cockerell 2012). Because melanoma in situ may remain asymptomatic and harmless, overdiagnosis can lead to unnecessary treatment (Bell and Nijsten 2022). The American Joint Committee on Cancer removed the Clark's level from its current staging system, as it is no longer considered a reliable classification for melanoma invasion depth.

Previous studies have reported plantar epidermal thickness; however, these measurements often aggregate into broader anatomical regions. Lintzeri et al. analyzed 37 skin areas using a meta-analysis and presented thickness as a single representative value per region (Lintzeri et al. 2022). Similarly, Lee and Hwang examined plantar skin thickness in Korean adults but reported it as a single measurement alongside 27 other skin sites (Lee and Hwang 2002). Although Chao et al. provided epidermal and total soft tissue thicknesses at five plantar points, a comprehensive analysis of the entire plantar region was lacking (Chao et al. 2011).

The site-specific skin and epidermal thickness data in this study provide a valuable reference for refining melanoma staging and optimizing excision depth and margins. Additionally, epidermal and dermal thicknesses may serve as predictive factors for melanoma invasion depth, aiding in the identification of affected skin layers based on the Breslow thickness.

Our results showed a mean total skin thickness of $1.71\pm0.31\,\mathrm{mm}$ and mean epidermal thickness of $0.55\pm0.12\,\mathrm{mm}$. The thinnest region was S4 (skin: $1.41\pm0.26\,\mathrm{mm}$, epidermis: $0.43\pm0.08\,\mathrm{mm}$), while the heel (S10 and S11) had the greatest thickness, with S11 showing the thickest skin $(2.19\pm0.29\,\mathrm{mm})$ and S10 the thickest epidermis $(0.71\pm0.14\,\mathrm{mm})$.

The medial arch (S4, S5, S7, and S8) consistently had the smallest thickness, whereas the thickness gradually increased from the medial to the lateral midfoot. The forefoot was thicker than the midfoot, but layer-specific variations were observed: S2 had the thickest total skin $(1.87\pm0.24\,\mathrm{mm})$, whereas its epidermis $(0.57\pm0.1\,\mathrm{mm})$ was thinner than S1 $(0.58\pm0.09\,\mathrm{mm})$ and S3 $(0.61\pm0.1\,\mathrm{mm})$. Among the toes, significant differences were noted: P1 $(1.77\pm0.21\,\mathrm{mm})$ and P2 $(1.71\pm0.17\,\mathrm{mm})$ resembled the forefoot in skin thickness, while P3 $(1.57\pm0.21\,\mathrm{mm})$ was closer to the medial arch. In the epidermis, P1 $(0.54\pm0.09\,\mathrm{mm})$ was similar to the lateral arch, whereas P2 $(0.51\pm0.07\,\mathrm{mm})$ and P3 $(0.49\pm0.09\,\mathrm{mm})$ resembled the medial arch.

These findings are consistent with those of previous studies on the plantar pressure distribution. Cavanagh et al. identified peak pressures across 10 anatomical regions with distinct weight distribution patterns (Cavanagh et al. 1987). Our results followed similar trends, demonstrating thicker skin and epidermis in the heel and forefoot, which bear high mechanical stress, and thinner skin and epidermis in the medial and lateral arches. Given the association between mechanical stress and plantar melanoma, variations in the thickness of high-pressure regions may have clinical relevance (Minagawa et al. 2016).

Age and sex are known to affect skin thickness (Shuster et al. 1975). In the present study, sex-related differences were observed only in dermal thickness, with no significant variations in total skin or epidermal thickness. No statistically significant correlation coefficient between age and thickness was identified, likely due to the uneven distribution of age groups (mostly <40 years or >70 years). However, epidermal thickness varied among the sample types, suggesting a possible age-related effect. Since type 3 (living individuals) were younger, while type 1 and 2 (cadavers) were older individuals, it is plausible that age affected epidermal thickness. Additionally, sex-related differences in skin thickness vary by anatomical region (Lee and Hwang 2002), and the inclusion of multiple plantar sites may have contributed to inconsistencies in sex-related findings.

Ultrasound is a reliable tool for assessing the plantar skin structure, allowing a precise localization of foot pathology and accurate thickness measurements (Filippini and Teh 2019). Its high resolution clearly differentiates the epidermis, dermis, and subcutaneous tissues, making it valuable for melanoma evaluation. The epidermis appears hyperechoic due to keratin, with a thick plantar stratum corneum forming a distinct bilaminar structure. The first echo marks the gel–stratum corneum interface, whereas the second corresponds to the base of the dermal papillae (Nouveau-Richard et al. 2004). Below the epidermis, the SLEB separates the papillary and reticular dermis (Nicolescu et al. 2023). The reticular dermis is hyperechoic but less bright than the epidermis because of its collagen content, whereas the subcutaneous tissue appears hypoechoic, reflecting fat lobules (Levy et al. 2021).

H&E and the Masson's trichrome staining help define each skin layer and reveal the microstructure of the skin, which agrees with the ultrasonographic findings. The Masson's trichrome staining, which stains collagen fibers blue, is used for the dermatopathological diagnosis and evaluation of connective tissues in skin specimens (Goldner 1938). By contrasting H&E staining with the Masson's trichrome staining, the assessment of the dermal structure that consisted of loose connective tissue of the papillary dermis and dense connective tissue of the reticular layer became clear. In some of the specimens, fibrous septa were detected in the subcutaneous tissue, which made it difficult to evaluate the thickness of the subcutaneous fat layer.

This study focused on epidermal and dermal thicknesses, excluding subcutaneous fat, which is clinically relevant for melanoma excision. Additionally, the lack of middle-aged participants limited age-related analysis, and the causal relationship between mechanical pressure and skin thickness was not directly examined, although the results aligned with those of previous plantar pressure studies. Future studies should further investigate biomechanical effects on plantar skin thickness to refine clinical guidelines.

5 | Conclusion

This study provides site-specific plantar skin thickness data and offers key insights into regional anatomical variations. The heel

had the greatest thickness, whereas the medial arch was the thinnest, mirroring the plantar pressure distributions and mechanical adaptations.

Given the substantial epidermal thickness of the plantar skin, relying solely on the Breslow thickness may overestimate the melanoma invasion depth, especially in cases confined to the epidermis or superficial layers. Integrating site-specific thickness data into clinical decision-making can refine melanoma staging and optimize excision strategies, ultimately enhancing diagnostic precision and improving patient outcomes.

Acknowledgments

The authors thank Hye-Won Huh from the Yonsei University College of Dentistry for assisting with the production of visual materials.

Consent

Informed consent was obtained from all subjects involved in the study.

Data Availability Statement

The datasets used and analyzed in this study are available from the corresponding author upon reasonable request.

References

Avry, F., C. Mousset, E. Oujagir, et al. 2022. "Microbubble-Assisted Ultrasound for Imaging and Therapy of Melanoma Skin Cancer: A Systematic Review." *Ultrasound in Medicine and Biology* 48, no. 11: 2174–2198.

Bell, K. J. L., and T. Nijsten. 2022. "Melanoma Overdiagnosis: Why It Matters and What Can Be Done About It." *British Journal of Dermatology* 187, no. 4: 459–460.

Boland, G. M., and J. E. Gershenwald. 2016. "Principles of Melanoma Staging." In *Melanoma*, edited by H. L. Kaufman and J. M. Mehnert, 131–148. Springer International Publishing.

Boyle, C. J., M. Plotczyk, S. F. Villalta, et al. 2019. "Morphology and Composition Play Distinct and Complementary Roles in the Tolerance of Plantar Skin to Mechanical Load." *Science Advances* 5, no. 10: eaay0244.

Brunicardi, F. C., D. K. Andersen, T. R. Billiar, et al. 2019. *Schwartz's Principles of Surgery*. McGraw-Hill Education.

Campillo-Recio, D., M. Ibañez, E. Jimeno-Torres, et al. 2021. "Two-Portal Endoscopic Plantar Fascia Release: Step-By-Step Surgical Technique." *Arthroscopy Techniques* 10, no. 1: e15–e20.

Cavanagh, P. R., M. M. Rodgers, and A. Iiboshi. 1987. "Pressure Distribution Under Symptom-Free Feet During Barefoot Standing." *Foot & Ankle 7*, no. 5: 262–276.

Chao, C. Y., Y. P. Zheng, and G. L. Cheing. 2011. "Epidermal Thickness and Biomechanical Properties of Plantar Tissues in Diabetic Foot." *Ultrasound in Medicine & Biology* 37, no. 7: 1029–1038.

Cockerell, C. J. 2012. "The Pathology of Melanoma." *Dermatologic Clinics* 30, no. 3: 445–468.

DeFazio, J. L., A. A. Marghoob, Y. Pan, S. W. Dusza, A. Khokhar, and A. Halpern. 2010. "Variation in the Depth of Excision of Melanoma: A Survey of US Physicians." *Archives of Dermatology* 146, no. 9: 995–999.

Filippini, C., and J. Teh. 2019. "Ultrasound Features of Sole of Foot Pathology: A Review." *Journal of Ultrasound* 19, no. 77: 145–151.

Fischer, J. E. 2019. "Fischer's Mastery of Surgery, 7e, ed. E.C.: Lippincott Williams & Wilkins, a Wolters Kluwer Business."

Fuchs, C., K. J. Stalnaker, C. L. Dalgard, et al. 2024. "Plantar Skin Exhibits Altered Physiology, Constitutive Activation of Wound-Associated Phenotypes, and Inherently Delayed Healing." *Journal of Investigative Dermatology* 144, no. 7: 1633–1648.e14.

Goldner, J. 1938. "A Modification of the Masson Trichrome Technique for Routine Laboratory Purposes." *American Journal of Pathology* 14, no. 2: 237–243.

Gui, J., Z. Guo, and D. Wu. 2022. "Clinical Features, Molecular Pathology, and Immune Microenvironmental Characteristics of Acral Melanoma." *Journal of Translational Medicine* 20, no. 1: 367.

Hashmi, F., C. Nester, C. Wright, V. Newton, and S. Lam. 2015. "Characterising the Biophysical Properties of Normal and Hyperkeratotic Foot Skin." *Journal of Foot and Ankle Research* 8: 35.

Hayashi, K., H. Koga, H. Uhara, and T. Saida. 2009. "High-Frequency 30-MHz Sonography in Preoperative Assessment of Tumor Thickness of Primary Melanoma: Usefulness in Determination of Surgical Margin and Indication for Sentinel Lymph Node Biopsy." *International Journal of Clinical Oncology* 14, no. 5: 426–430.

Jung, H. J., S. S. Kweon, J. B. Lee, S. C. Lee, and S. J. Yun. 2013. "A Clinicopathologic Analysis of 177 Acral Melanomas in Koreans: Relevance of Spreading Pattern and Physical Stress." *JAMA Dermatology* 149, no. 11: 1281–1288.

Koshenkov, V. P., J. Broucek, and H. L. Kaufman. 2016. "Surgical Management of Melanoma." In *Melanoma*, edited by H. L. Kaufman and J. M. Mehnert, 149–179. Springer International Publishing.

Lee, Y., and K. Hwang. 2002. "Skin Thickness of Korean Adults." Surgical and Radiologic Anatomy 24, no. 3–4: 183–189.

Levy, J., D. L. Barrett, N. Harris, J. J. Jeong, X. Yang, and S. C. Chen. 2021. "High-Frequency Ultrasound in Clinical Dermatology: A Review." *Ultrasound Journal* 13, no. 1: 24.

Lillemoe, H. A., J. K. Williams, M. K. Teshome, et al. 2023. "Setting the Standard for Cutaneous Melanoma Wide Local Excision: An Overview of the American College of Surgeons Commission on Cancer Standard 5.5." *Journal of the American College of Surgeons* 236, no. 2: 424–428.

Lintzeri, D. A., N. Karimian, U. Blume-Peytavi, and J. Kottner. 2022. "Epidermal Thickness in Healthy Humans: A Systematic Review and Meta-Analysis." *Journal of the European Academy of Dermatology and Venereology* 36, no. 8: 1191–1200.

Long, G. V., S. M. Swetter, A. M. Menzies, J. E. Gershenwald, and R. A. Scolyer. 2023. "Cutaneous Melanoma." *Lancet* 402, no. 10400: 485–502.

Loscalzo, J., A. Fauci, D. Kasper, et al. 2022. *Harrison's Principles of Internal Medicine*. McGraw-Hill Education.

Machet, L., V. Belot, M. Naouri, et al. 2009. "Preoperative Measurement of Thickness of Cutaneous Melanoma Using High-Resolution 20 MHz Ultrasound Imaging: A Monocenter Prospective Study and Systematic Review of the Literature." *Ultrasound in Medicine and Biology* 35, no. 9: 1411–1420.

Minagawa, A., T. Omodaka, and R. Okuyama. 2016. "Melanomas and Mechanical Stress Points on the Plantar Surface of the Foot." *New England Journal of Medicine* 374, no. 24: 2404–2406.

Morrison, T., S. Jones, R. S. Causby, and K. Thoirs. 2021. "Reliability of Ultrasound in Evaluating the Plantar Skin and Fat Pad of the Foot in the Setting of Diabetes." *PLoS One* 16, no. 9: e0257790.

Nicolescu, A. C., S. Ionescu, I. Ancuta, et al. 2023. "Subepidermal Low-Echogenic Band-Its Utility in Clinical Practice: A Systematic Review." *Diagnostics* 13, no. 5: 970.

Nouveau-Richard, S., M. Monot, P. Bastien, and O. de Lacharrière. 2004. "In Vivo Epidermal Thickness Measurement: Ultrasound vs. Confocal Imaging." *Skin Research and Technology* 10, no. 2: 136–140.

8 Clinical Anatomy, 2025

- Rager, E. L., E. P. Bridgeford, and D. W. Ollila. 2005. "Cutaneous Melanoma: Update on Prevention, Screening, Diagnosis, and Treatment." *American Family Physician* 72, no. 2: 269–276.
- Sellyn, G. E., A. A. Lopez, S. Ghosh, et al. 2025. "High-Frequency Ultrasound Accuracy in Preoperative Cutaneous Melanoma Assessment: A Meta-Analysis." *Journal of the European Academy of Dermatology and Venereology* 39, no. 1: 86–96.
- Seo, J., H. S. Kim, K. I. Min, et al. 2022. "Weight-Bearing Activity Impairs Nuclear Membrane and Genome Integrity via YAP Activation in Plantar Melanoma." *Nature Communications* 13, no. 1: 2214.
- Shuster, S., M. M. Black, and E. McVitie. 1975. "The Influence of Age and Sex on Skin Thickness, Skin Collagen and Density." *British Journal of Dermatology* 93, no. 6: 639–643.

Van Boerum, D. H., and B. J. Sangeorzan. 2003. "Biomechanics and Pathophysiology of Flat Foot." *Foot and Ankle Clinics* 8, no. 3: 419–430.